Fast Data-Driven Calibration of a Cardiac Electrophysiology Model from Images and ECG

Oliver Zettinig[1,2], Tommaso Mansi[1], Bogdan Georgescu[1], Elham Kayvanpour[3], Farbod Sedaghat-Hamedani[3], Ali Amr[3], Jan Haas[3], Henning Steen[3], Benjamin Meder[3], Hugo Katus[3], Nassir Navab[2], Ali Kamen[1], and Dorin Comaniciu[1]

[1] Siemens Corporation, Corporate Technology, Imaging and Computer Vision, Princeton, NJ, USA
[2] Computer Aided Medical Procedures, Technische Universität München, Germany
[3] University Hospital Heidelberg, Department of Internal Medicine III - Cardiology, Angiology and Pneumology, Heidelberg, Germany

Abstract. Recent advances in computational electrophysiology (EP) models make them attractive for clinical use. We propose a novel data-driven approach to calibrate an EP model from standard 12-lead electrocardiograms (ECG), which are in contrast to invasive or dense body surface measurements widely available in clinical routine. With focus on cardiac depolarization, we first propose an efficient forward model of ECG by coupling a mono-domain, Lattice-Boltzmann model of cardiac EP to a boundary element formulation of body surface potentials. We then estimate a polynomial regression to predict myocardium, left ventricle and right ventricle endocardium electrical diffusion from QRS duration and ECG electrical axis. Training was performed on 4,200 ECG simulations, calculated in $\approx 3\,s$ each, using different diffusion parameters on 13 patient geometries. This allowed quantifying diffusion uncertainty for given ECG parameters due to the ill-posed nature of the ECG problem. We show that our method is able to predict myocardium diffusion within the uncertainty range, yielding a prediction error of less than $5\,ms$ for QRS duration and 2° for electrical axis. Prediction results compared favorably with those obtained with a standard optimization procedure, while being 60 times faster. Our data-driven model can thus constitute an efficient preliminary step prior to more refined EP personalization.

1 Introduction

With the improvement in patient care after myocardium infarction or cardiomyopathies, the prevalence of cardiac rhythm disorders has increased significantly [1]. Electrocardiography (ECG) is the preferred tool to assess arrhythmias, conduction abnormalities and the effects of treatments on the electrical activity of the heart. However, with the development of non-invasive treatments, more detailed and predictive electrophysiology (EP) assessment is necessary [1].

The last decade has seen tremendous progress in computational modeling of cardiac EP [2]. Recent numerical methods are enabling near real-time EP

computation [3, 4]. To be applied in clinical practice, these models need to be adjusted to capture patient physiology. Current approaches use inverse problem methods to estimate electrical diffusivity or action potential duration from invasive endocardial mapping [5] or body surface mapping (BSM) [6, 7]. However, these methods are computationally demanding as they require hundreds of forward model runs. Another limitation is the lack of availability of these diagnostic modalities: invasive measurements are often avoided, whereas BSM is still not widely available. Methods based on standard ECG would therefore constitute good alternatives when comprehensive EP information is not available.

At the same time, efficient machine learning algorithms have been developed for medical applications. First applied for anatomy detection and segmentation [8], applications for model personalization are now being investigated. In [9], the authors derived a surrogate EP model based on polynomial chaos theory to personalize an Eikonal model and quantify parameter uncertainty. Statistical learning has also been employed to back-project BSM potentials onto the epicardium [10]. Provided the parameter space is sufficiently sampled, statistical learning can constitute an efficient approach for model personalization.

In this context, we propose a novel method to calibrate a cardiac EP model based on commonly available 12-lead ECG measurements. As a first step, we focus on cardiac depolarization and aim at estimating ventricular electrical diffusion only, the other EP parameters being fixed to their nominal values. To be able to scan the parameter space, we introduce a novel ECG model based on a mono-domain, Lattice-Boltzmann EP model. Then, we use a data-driven approach to estimate a polynomial regression whose predictors are standard ECG parameters (QRS duration, electrical axis) and responses are myocardium diffusivity parameters (Sec. 2). Thanks to the computational efficiency of our framework, we show in Sec. 3 that our approach is able to reach the intrinsic uncertainty of the problem, which could be quantitatively estimated from 4,200 forward simulations. The proposed method also compared favorably with NEWUOA [5], a standard inverse problem algorithm, and yielded promising results on three patient data. As discussed in Sec. 4, our data-driven approach may constitute a preliminary calibration step for patient-specific EP modeling.

2 Method

2.1 Fast Forward Model of Cardiac ECG

Patient-Specific Model of Cardiac Anatomy The first step of our approach consists in segmenting the heart geometry from clinical images (Fig. 1). A robust, data-guided machine learning algorithm is employed to automatically segment cardiac chambers and epicardium from cine MRI images [8]. Next, the biventricular myocardium domain at end-diastasis is mapped onto a Cartesian grid and represented as a level-set. Finally, fiber architecture is calculated by following a rule-based approach [3]: Below the basal plane, fiber elevation angles vary linearly from epi- ($-70°$) to endocardium ($+70°$), which are then extrapolated up to the valves based on geodesic distance (Fig. 2b). The heart is registered to a

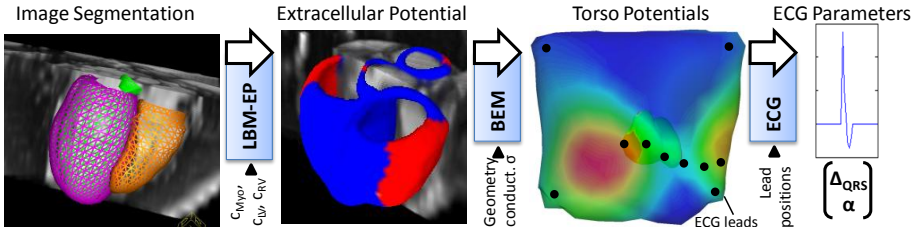

Fig. 1. Steps of proposed forward model of ECG. *See text for details.*

torso atlas using Procrustes analysis. The entire pipeline is fully automatic but under expert guidance to allow manual corrections.

Lattice-Boltzmann Model of Myocardium Transmembrane Potentials As the proposed data-driven model relies on global ECG information, simplified mono-domain EP methods can be employed, since they have been shown to preserve the essential ECG features well [11, 12]. In this work, the trans-membrane potential (TMP) $v(t) \in [-70\,mV, 30\,mV]$ is calculated according to the Mitchell-Schaeffer model (see [3, 13] and references therein):

$$\frac{\partial v}{\partial t} = \frac{h(t)v^2(1-v)}{\tau_{in}} - \frac{v}{\tau_{out}} + c\nabla \cdot D\nabla v \tag{1}$$

$h(t)$ is a gating variable that models the state of the ion channels ($dh/dt = (1-h)/\tau_{open}$ if $v < v_{gate}$, $dh/dt = -h/\tau_{close}$ otherwise). c is the tissue diffusivity whose anisotropy is captured by the tensor D. The τ's and v_{gate} are parameters that control the dynamics of the action potential. This complex PDE is solved using the LBM-EP method [3], an efficient Lattice-Boltzmann algorithm. Five domains are considered: left and right ventricular septum, used to pace the heart to mimic the His bundle; left and right endocardia with fast electrical diffusivity, c_{LV} and c_{RV}, to mimic the Purkinje network; and the myocardium, with slower diffusivity c_{Myo} (Fig. 2b).

Boundary Element Model of Torso Potentials Torso potentials are calculated in three steps. First, extra-cellular potentials are estimated from the TMP by using the elliptic formulation proposed in [12], where the diffusion anisotropy ratio $c_i(\mathbf{x})/c_e(\mathbf{x}) = \lambda$ is assumed constant ($\mathbf{x}$ is the spatial position, c_i and c_e are the intra-cellular and extra-cellular diffusion coefficients respectively). With that hypothesis, the extra-cellular potential ϕ_e writes:

$$\phi_e(\mathbf{x}, t) = \frac{\lambda}{1+\lambda} \frac{1}{|\Omega|} \int_{\Omega} (v(\mathbf{y}, t) - v(\mathbf{x}, t)) d\mathbf{y} \tag{2}$$

Ω is the entire myocardium domain. Second, ϕ_e is mapped back to the epicardium surface mesh S_H using tri-linear interpolation. Finally, the extra-cellular potentials are projected onto the torso surface S_B using a boundary element method (BEM) [14]. The potential $\phi(\mathbf{x})$ at any point $\mathbf{x}$ of the thoracic domain writes, in virtue of Green's second identity,

$$\phi(\mathbf{x}) = \frac{1}{4\pi} \int_{S_B} \phi_B \frac{\mathbf{r} \cdot \mathbf{n}}{||\mathbf{r}||^3} dS_B - \frac{1}{4\pi} \int_{S_H} \left[\phi_e \frac{\mathbf{r} \cdot \mathbf{n}}{||\mathbf{r}||^3} + \frac{\nabla \phi_e \cdot \mathbf{n}}{||\mathbf{r}||} \right] dS_H \tag{3}$$

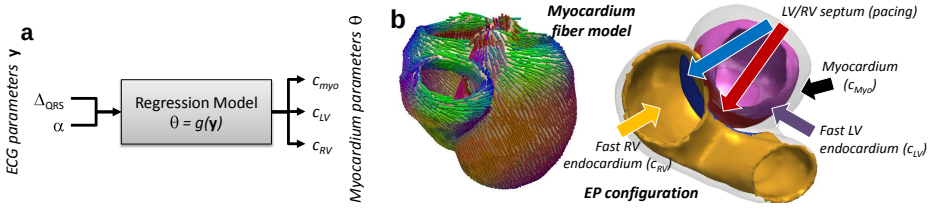

Fig. 2. a) Schematic diagram of the data-driven backward ECG model. **b)** Myocardium fiber model in one patient and EP configuration. *See text for details.*

where $\mathbf{r}$ is the vector defined by $\mathbf{x}$ and the integration point. By discretizing S_B and S_H into triangulations, the linear systems $\mathrm{P}_{BB}\,\phi_B + \mathrm{P}_{BH}\,\phi_e + \mathrm{G}_{BH}\,\Gamma_H = 0$ and $\mathrm{P}_{HB}\,\phi_B + \mathrm{P}_{HH}\,\phi_e + \mathrm{G}_{HH}\,\Gamma_H = 0$ can be constructed. The matrices P and G contain coefficients depending entirely on the geometry, and can therefore be precomputed, while the matrix Γ_H collects the gradients $\nabla\phi_H$. Finally, ϕ on the body is given by $\phi_B = \left(P_{BB} - G_{BH}G_{HH}^{-1}P_{HB}\right)^{-1}\left(G_{BH}G_{HH}^{-1}P_{HH} - P_{BH}\right)\phi_e$.
ECG Calculation We finally compute the standard Einthoven, Goldberger and Wilson leads, and derive the QRS duration Δ_{QRS} and mean electrical axis angle α automatically. The QRS complex is detected as in [15] by convolving the squared derivative of each limb lead $y_f(t) = [d/dt\, y(t)]^2$ with a sliding average kernel (window size $24\,ms$) for increased robustness. A threshold value of $0.8\,mV^2ms^{-2}$ has proven to be sufficient for detecting Δ_{QRS}. The electrical axis is computed based on the leads I and II: $\alpha = \arctan((2h_{II} - h_I)/(\sqrt{3}h_I))$, where the h_i's are the sum of R and S peak amplitudes in the respective leads.

2.2 Data-Driven Estimation of Myocardium EP Diffusion

The forward ECG model can be seen as a dynamic system $\mathbf{y} = f(\theta)$. In this work, the free parameters θ are the diffusivity values, $\theta = (c_{Myo}, c_{LV}, c_{RV})$, whereas the outputs $\mathbf{y}$ are the ECG parameters, $\mathbf{y} = (\Delta_{QRS}, \alpha)$, which are often available from ECG traces (Fig. 2). Calibrating the EP model thus consists in evaluating a function $g(\mathbf{y})$ that approximates the inverse problem $\theta = g(\mathbf{y}) \approx f^{-1}(\mathbf{y})$.

Δ_{QRS} and α can vary significantly within the population, even in normal subjects, due to heart morphology, position, and other factors not directly related to myocardium diffusivity. To cope with these variabilities, we normalize Δ_{QRS} and α by scouting the space of possible values by means of three forward simulations: one with normal diffusivity parameters (F_1: $c_{LV} = c_{RV} = 16,000\,mm^2/s$, $c_{Myo} = 6,000\,mm^2/s$), one with low LV diffusivity (LBBB-like scenario, F_2: $c_{LV} = 1,200\,mm^2/s$, $c_{RV} = 16,000\,mm^2/s$, $c_{Myo} = 1,000\,mm^2/s$) and one with low RV diffusivity (RBBB-like scenario, F_3, the other way round). The normalized parameters are then defined by $\overline{\Delta_{QRS}} = \Delta_{QRS}/\Delta_{QRS_{F_1}}$ and $\overline{\alpha} = (\alpha - \alpha_{F_2})/(\alpha_{F_3} - \alpha_{F_2})$. By doing so, the ECG parameters are relative to a nominal, patient-specific simulation, which intrinsically considers patient geometry features. Finally, we learn the model $\theta = g(\overline{\Delta_{QRS}}, \overline{\alpha})$ by using multivariate polynomial regression method of degree seven [16], which offered a good

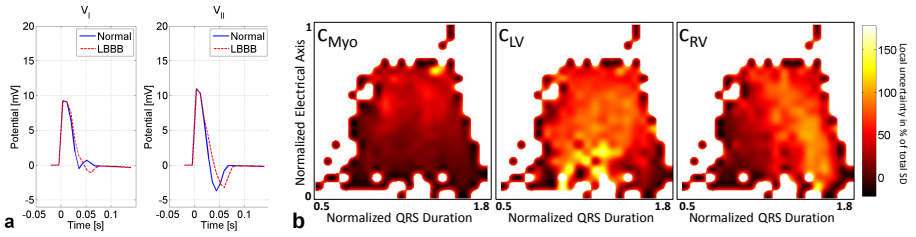

Fig. 3. a) QRS complex in simulated limb ECG leads V_I and V_{II} in normal and left bundle branch block physiology (LBBB). Our model was able to capture longer QRS due to delayed depolarization in LBBB. **b)** Estimated diffusion standard deviation (SD) in % of total SD for known electrical axis and QRS duration. The highest uncertainty is found in the healthy range of parameters (center of plots).

compromise between prediction accuracy and generalization (no significant differences in performance could be distinguished with orders varying from 4 to 9). In this work, one regression function is learned for each diffusivity parameter independently, $\mathbf{g} = (g_{Myo}, g_{LV}, g_{RV})$. We also investigated multivariate regression splines (MARS) and gradient boosting, which yielded very similar results. After having trained $\mathbf{g}$, the diffusivity parameters are estimated from the measured and normalized ECG features: $(c_{\hat{Myo}}, c_{\hat{LV}}, c_{\hat{RV}}) = \mathbf{g}(\overline{\Delta_{QRS}}, \overline{\alpha})$.

3 Experiments and Results

3.1 Forward ECG Model Evaluation and Uncertainty Analysis

Experimental Protocol Thirteen dilated cardiomyopathy (DCM) patients were used, for which an anatomical model was automatically created based on cine MRI images. Then, a total of 4,200 EP simulations were generated on a $1.5\,mm$ isotropic Cartesian grid with diffusivity coefficients uniformly sampled between $1,000\,mm^2/s$ and $16,000\,mm^2/s$ under the constraints $c_{Myo} \leq c_{LV}$ and $c_{Myo} \leq c_{RV}$. Electrode positions were chosen to coincide with appropriate vertex positions. Implemented on GPU (NVIDIA GeForce GTX 580), the model could compute the ECG of one cardiac cycle in $\approx 3\,s$.

Forward Model Evaluation Normal EP was modeled in one dataset with $c_{LV} = c_{RV} = 16,000\,mm^2/s$, $c_{Myo} = 1,000\,mm^2/s$ (Fig. 1, second panel). A left bundle branch block (LBBB) scenario was mimicked by setting $c_{LV} = 5,000\,mm^2/s$. As one can see from Fig. 3a, R and S wave trends were qualitatively realistic. In particular, the model was able to capture prolonged QRS due to the slow conduction in the LBBB case. As our model concentrates on the ventricular EP only, calculated ECG did not incorporate P waves. Missing Q waves could also be explained by the absence of His bundle excitation in our EP model, as the whole septum area is triggered (Sec. 2.1). Experiments with different fiber angles ($-50/50°$, $-70/70°$, $-90/90°$) showed that the QRS duration remains constant and the electrical axis stays in the diagnostically same range for pathological configurations F_2 and F_3 with a standard deviation of 15.8°.

Uncertainty Analysis Based on the 4,200 simulations, we analyzed the intrinsic uncertainty of the ECG inverse problem, i.e. the uncertainty in cardiac diffusion parameters given Δ_{QRS} and α. For that study, normalized values (Sec. 2.2) were used to minimize the effects of geometry. Each (Δ_{QRS}, α) pairs were grouped in 20×20 bins. For each bin, the standard deviation (SD) of c_{Myo}, c_{LV} and c_{RV} was calculated. Total SD over the entire dataset was $2,146\,mm^2/s$, $4,142\,mm^2/s$ and $4,123\,mm^2/s$ respectively. Fig. 3b reports the local SD per bin in % of the total SD. The local SD is on average 20%, 52% and 40% of the total SD for c_{Myo}, c_{LV} and c_{RV} respectively, with up to 150% of variation. Interestingly, similar variations were obtained patient-wise. These results clearly reflect the ill-posed nature of the ECG inverse problem under our forward model and constitute first estimates of the optimal bound in accuracy for any inverse problem to estimate myocardium diffusion that rely on Δ_{QRS} and α only. The uncertainty may decrease if more ECG parameters are considered.

3.2 Evaluation of the Data-Driven Calibration Model

Evaluation on Synthetic Data Our model was evaluated using leave-one-patient-out cross-validation. On average, c_{Myo} could be estimated within 23% of the total SD, while c_{LV} and c_{RV} were predicted within 56% and 55% respectively, i.e. up to the intrinsic uncertainty of the problem. Without normalization, errors were betwen 114% and 440% of the total SD. The proposed model-based normalization procedure was thus able to compensate for inter-patient geometry variability. To evaluate the accuracy of the regression model in the observable space of ECG parameters, Δ_{QRS} and α computed by the calibrated forward model were compared with the known ground truth. As illustrated in Fig. 4a-b, an average error of $4.9 \pm 5.5\,ms$ for Δ_{QRS} (mean $\pm$ SD) and $1.6 \pm 1.7^\circ$ for α was obtained. These errors were in the range of clinical variability. Moreover, calibrated simulations were significantly (t-test p-value < 0.001) more precise than those obtained with nominal diffusivity values (Δ_{QRS} error: $19.8 \pm 14.3\,ms$, α error: $4.3 \pm 3.4^\circ$). Additionally, while our prediction was on average centered around the ground truth QRS duration (average bias: $+0.5\,ms$), the Δ_{QRS} calculated with default parameters was $19.0\,ms$ too short. This result was expected since the default parameters correspond to healthy physiology whereas conduction abnormalities cause prolonged QRS durations. Using our calibration technique may thus be preferable to using nominal parameters when only ECG is available.

Comparison with NEWUOA We compared the performance of the regression model with those obtained with NEWUOA [5], a gradient-free inverse problem method. The cost function was defined as $f(\Delta^i_{QRS}, \alpha^i) = (\Delta^{known}_{QRS} - \Delta^i_{QRS})^2 + \lambda(\alpha^{known} - \alpha^i)^2$ with $\lambda = 0.1$ to account for the different orders of magnitude between ECG parameters. Similarly to our regression model, tissue diffusivities c_{Myo}, c_{LV} and c_{RV} could be estimated within 23%, 64% and 54% of the total SD, respectively, which was also close to the limit of data uncertainty. Errors in Δ_{QRS} and α calculated using the NEWUOA-personalized forward model were on average $8.7 \pm 11.1\,ms$ (significantly biased compared to our approach) and $-0.2 \pm 7.6^\circ$ respectively. From a computational point of view, NEWUOA took

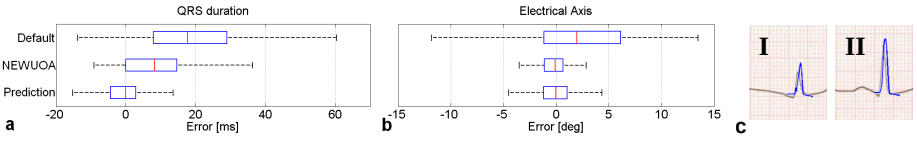

Fig. 4. a, b) QRS duration and electrical axis error distributions for ECG simulations with nominal (top), NEWUOA-predicted (center) and regression-predicted (bottom) diffusivity parameters. Our approach yielded more accurate predictions. **c)** Measured (*black*) and simulated (*blue*) V_I and V_{II} leads after model calibration for one patient.

about $10\,min$ to converge, while our approach required only $10\,s$ to calculate the three forward simulations for the normalization. Hence, our approach not only yielded more predictive calibrations but was also $60\times$ more efficient.

Evaluation on Real Cases The method was finally evaluated on four DCM patients for which clinical ECG was available. Diffusivity parameters were estimated based on measured QRS duration and electrical axis angle using the trained regression model. For one patient, myocardium diffusivity could not be calibrated as the measured electrical axis ($\alpha = -63°$) was outside the range of the training set. However, for the three other patients, plausible diffusion coefficients could be estimated ($2426 - 7584\,mm^2/s$ for c_{Myo}, and $6691 - 12532\,mm^2/s$ for c_{LV} and c_{RV}). We then calculated the ECG using the calibrated forward model, yielding a promising average error of $0.35 \pm 0.28\,ms$ for Δ_{QRS} and $15.6° \pm 9.6°$ for α respectively. Fig. 4c illustrates the calculated ECG overlaid on top of the real ECG for one patient, showing promising agreement.

4 Conclusion and Future Work

In this paper, we have shown that the calibration of patient-specific cardiac electrophysiology models is possible from standard 12-lead ECG measurements. By learning a data-driven regression model from simulated ECG signals, we were able to predict diffusivity parameters for various regions of the myocardium, up to the limit of the underlying uncertainty due to the intrinsic ill-posedness of the inverse ECG problem. We could also, for the first time to the best of our knowledge, quantify the uncertainty in estimated myocardium diffusion when only ECG data is employed, under the assumptions of our forward model. Experiments with synthetic ECG data and four patients showed promising results, with significant improvement with respect to nominal diffusivity values and better predictive power compared to NEWUOA calibration. Thus, our method can provide good preliminary personalization, prior to more refined estimation if invasive or BSM measurements are available. Future extensions of our framework include the analysis of the entire ECG trace, improved capture of geometrical features, refinement of the forward model to include more sophisticated activation patterns and other parameters of the EP model, and non-linear manifold learning to improve the performances on unseen data. In addition, an electromechanical model of the heart currently under development will help us in quantifying the error introduced by assuming a static myocardium.

References

1. Marcus, G.M., Keung, E., Scheinman, M.M.: The year in review of cardiac electrophysiology. JACC 61(7), 772–782 (2013)
2. Clayton, R.H., Bernus, O., Cherry, E.M., Dierckx, H., Fenton, F.H., Mirabella, L., Panfilov, A.V., Sachse, F.B., Seemann, G., Zhang, H.: Models of cardiac tissue electrophysiology: Progress, challenges and open questions. PBMB 104(1), 22–48 (2011)
3. Rapaka, S., Mansi, T., Georgescu, B., Pop, M., Wright, G., Kamen, A., Comaniciu, D.: LBM-EP: Lattice-Boltzmann method for fast cardiac electrophysiology simulation from 3D images. In: Ayache, N., Delingette, H., Golland, P., Mori, K. (eds.) MICCAI 2012, Part II. LNCS, vol. 7511, pp. 33–40. Springer, Heidelberg (2012)
4. Talbot, H., Marchesseau, S., Duriez, C., Sermesant, M., Cotin, S., Delingette, H.: Towards an interactive electromechanical model of the heart. Int. Focus 3(2) (2013)
5. Relan, J., Chinchapatnam, P., Sermesant, M., Rhode, K., Ginks, M., Delingette, H., Rinaldi, C.A., Razavi, R., Ayache, N.: Coupled personalization of cardiac electrophysiology models for prediction of ischaemic ventricular tachycardia. Int. Focus 1(3), 396–407 (2011)
6. Dössel, O., Krueger, M., Weber, F., Schilling, C., Schulze, W., Seemann, G.: A framework for personalization of computational models of the human atria. In: Proc. EMBC 2011, IEEE, pp. 4324–4328 (2011)
7. Wang, L., Wong, K.C., Zhang, H., Liu, H., Shi, P.: Noninvasive computational imaging of cardiac electrophysiology for 3-d infarct. IEEE TBE 58(4), 1033 (2011)
8. Zheng, Y., Barbu, A., Georgescu, B., Scheuering, M., Comaniciu, D.: Four-chamber heart modeling and automatic segmentation for 3-D cardiac CT volumes using marginal space learning and steerable features. IEEE TMI 27(11), 1668–1681 (2008)
9. Konukoglu, E., Relan, J., Cilingir, U., Menze, B.H., Chinchapatnam, P., Jadidi, A., Cochet, H., Hocini, M., Delingette, H., Jaïs, P., Haïssaguerre, M., Ayache, N., Sermesant, M.: Efficient probabilistic model personalization integrating uncertainty on data and parameters: Application to Eikonal-diffusion models in cardiac electrophysiology. PBMB 107(1), 134–146 (2011)
10. Jiang, M., Lv, J., Wang, C., Huang, W., Xia, L., Shou, G.: A hybrid model of maximum margin clustering method and support vector regression for solving the inverse ECG problem. Computing in Cardiology, 2011. pp. 457–460 (2011)
11. Boulakia, M., Cazeau, S., Fernández, M.A., Gerbeau, J.-F., Zemzemi, N.: Mathematical modeling of electrocardiograms: a numerical study. Ann Biomed Eng 38(3), 1071–1097 (2010)
12. Chhay, M., Coudière, Y., Turpault, R.: How to compute the extracellular potential in electrocardiology from an extended monodomain model. RR-7916, INRIA 2012
13. Mitchell, C., Schaeffer, D.: A two-current model for the dynamics of cardiac membrane. Bull Math Biol 65(5), 767–793 (2003)
14. Shou, G., Xia, L., Jiang, M., Wei, Q., Liu, F., Crozier, S.: Solving the ECG forward problem by means of standard H- and H-hierarchical adaptive linear boundary element method. IEEE TBE 56(5), 1454 –1464 (2009)
15. Kohler, B.U., Hennig, C., Orglmeister, R.: The principles of software QRS detection. Engineering in Medicine and Biology Magazine, IEEE 21(1), 42–57 (2002)
16. Friedman, J., Hastie, T., Tibshirani, R.: The Elements of Statistical Learning: Data Mining, Inference, and Prediction. Springer (2009)